

NON-BIFURCATING PHYLOGENETIC TREE INFERENCE VIA THE ADAPTIVE LASSO

CHENG ZHANG^{1*}, VU DINH^{2*}, AND FREDERICK A. MATSEN IV¹

ABSTRACT. Phylogenetic tree inference using deep DNA sequencing is reshaping our understanding of rapidly evolving systems, such as the within-host battle between viruses and the immune system. Densely sampled phylogenetic trees can contain special features, including *sampled ancestors* in which we sequence a genotype along with its direct descendants, and *polytomies* in which multiple descendants arise simultaneously. These features are apparent after identifying zero-length branches in the tree. However, current maximum-likelihood based approaches are not capable of revealing such zero-length branches. In this paper, we find these zero-length branches by introducing adaptive-LASSO-type regularization estimators to phylogenetics, deriving their properties, and showing regularization to be a practically useful approach for phylogenetics.

Keywords: phylogenetics, ℓ_1 regularization, adaptive LASSO, sparsity, model selection, consistency, FISTA

1. INTRODUCTION

Phylogenetic methods, originally developed to infer evolutionary relationships among species separated by millions of years, are now widely used in biomedicine to investigate very short-time-scale evolutionary history. For example, mutations in viral genomes can inform us about patterns of infection and evolutionary dynamics as they evolve in their hosts on a time-scale of years (Grenfell et al., 2004). Antibody-making B cells diversify in just a few weeks, with a mutation rate around a million times higher than the typical mutation rate for cell division (Kleinstein et al., 2003). Although general-purpose phylogenetic methods have proven useful in these biomedical settings, the basic assumption that evolutionary trees follow a bifurcating pattern need not hold. Our goal is to develop a penalized maximum-likelihood approach to infer non-bifurcating trees (Figure 1).

Although our practical interests concern inference for finite-length sequence data, some situations in biology will lead to non-bifurcating phylogenetic trees, even in the theoretical limit of infinite sequence information. For example, a retrovirus such as HIV incorporates a copy of its genetic material into the host cell upon infection. This genetic material is then used for many copies of the virus, and when more than two descendants from this infected cell are then sampled for sequencing, the correct phylogenetic tree forms a multifurcation from these multiple descendants (a.k.a. a *polytomy*). In other situations we may sample an ancestor along with a descendant cell, which will appear as a node with a single descendant

* Equal contribution, ¹Fred Hutchinson Cancer Research Center, ²University of Delaware.

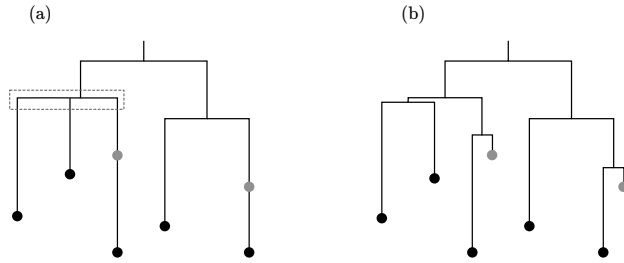


FIGURE 1. (a) A cartoon evolutionary scenario, with sampled ancestors (gray dots) and a multifurcation (dashed box). (b) A corresponding standard maximum likelihood phylogenetic inference, without regularization or thresholding.

edge (Figure 1). For example, antibody-making B cells evolve within host in dense accretions of cells called germinal centers in order to better bind foreign molecules (Victora and Nussenzweig, 2012). In such settings it is possible to sample a cell along with its direct descendant. Indeed, upon DNA replication in cell division, one cell inherits the original DNA of the coding strand, while the other inherits a copy which may contain a mutation from the original. If we sequence both of these cells, the first cell is the genetic ancestor of the second cell for this coding region. In this case the correct configuration of the two genotypes is that the first cell is a *sampled ancestor* of the second cell.

However DNA sequences are finite and often rather short, limiting the amount of information available with which to infer phylogenetic trees. Even though entire genomes are large, the segment of interest for a phylogenetic analysis is frequently small. For example, B cells evolve rapidly only in the hundreds of DNA sites used to encode antibodies, and thus sequencing is typically applied only to this region (Georgiou et al., 2014). Similarly, modern applications of pathogen outbreak analysis using sequencing (Gardy et al., 2015) frequently observe the same sequence, indicating that sampling is dense relative to mutation rates. Because genetic recombination and processes such as viral reassortment (Chen and Holmes, 2008) break the assumption that genetic data has evolved according to a single tree, practitioners often restrict analysis to an even shorter region that they believe has evolved according to a single process.

Inference on these shorter sequences further motivates correct inferences for non-bifurcating tree inference. Indeed, even if a collection of sequences in fact did diverge in a bifurcating fashion, if no mutations happened in the sequenced region during this diversification (i.e. a zero-length branch) then a non-bifurcating representation is appropriate. We thus expect multifurcations and sampled ancestors whenever the interval between the bifurcations is short compared to the total mutation rate in the sequenced region.

Non-bifurcating tree inference has thus far been via Bayesian phylogenetics, with the two deviations from bifurcation in two separate lines of work. For multifurcations, Lewis et al. (2005, 2015) develop a prior on phylogenetic trees with positive mass on multifurcating trees, and then perform tree estimation using reversible jump MCMC (rjMCMC) moves between trees. For sampled ancestors, Gavryushkina et al. (2014, 2016) introduce a prior on trees with sampled ancestors and then

also use rjMCMC for inference. To our knowledge no priors have been defined that place mass on trees with both multifurcations or sampled ancestors.

Current biomedical applications require a more computationally efficient alternative than these Bayesian techniques. Indeed, current methods for real-time phylogenetics in the course of a viral outbreak use maximum likelihood (Neher and Bedford, 2015; Libin et al., 2017), which is orders of magnitude faster than Bayesian analyses. This is essential because the time between new sequences being added to the database is shorter than the required execution time for a Bayesian analysis. However, to our knowledge a maximum-likelihood alternative to such rjMCMC phylogenetic inference for multifurcating trees does not yet exist.

Elsewhere in statistics, researchers find zero sets of parameters via penalized maximum likelihood inference, commonly maximizing the sum of a penalty term and a log likelihood function. When the penalty term has a nonzero slope as each variable approaches zero, the penalty will have the effect of “shrinking” that variable to zero when there is not substantial evidence from the likelihood function that it should be nonzero. There is now a substantial literature on such estimators, of which L_1 penalized estimators such as LASSO (Tibshirani, 1996) are the most popular.

In this paper, we introduce such regularization estimators into phylogenetics, derive their properties, and show regularization to be a practically-useful approach for phylogenetics via new algorithms and experiments. Specifically, we first show consistency: that the LASSO and its adaptive variants find all zero-length branches in the limit of long sequences with an appropriate penalty weight. We also derive new algorithms for phylogenetic LASSO and show them to be effective via simulation experiments and application to a Dengue virus data set.

Phylogenetic LASSO is challenging and requires additional new techniques above those for classical LASSO. First, the phylogenetic log-likelihood function is non-linear and non-convex. More importantly, unlike the standard settings for model selection where the variables can receive both positive and negative values, the branch lengths of a tree are non-negative. Thus, the objective function of phylogenetic LASSO can only be defined on a constrained compact space, for which the “true parameter” lies on the boundary of the domain. Furthermore the behavior of the phylogenetic log-likelihood on this boundary is untamed: when multiple branch lengths of a tree approach zero at the same time, the log-likelihood function may diverge to infinity, even if it is analytic in the inside of the domain of definition. The geometry of the subset of the boundary where these singularities happen is non-trivial, especially in the presence of randomness in data. All of these issues combine to make theoretical analyses and practical implementation of these estimators an interesting challenge.

2. MATHEMATICAL FRAMEWORK

2.1. Phylogenetic tree. A *phylogenetic tree* is a tree graph τ such that each leaf has a unique name, and such that each edge e of the tree is associated with a non-negative number q_e . We will denote by E and V the set of edges and vertices of the tree, respectively. We will refer to τ and $(q_e)_{e \in E}$ as the *tree topology* and the *vector of branch lengths*, respectively. Any edge adjacent to a leaf is called a pendant edge, and any other edge is called an internal edge. A pendant edge with

zero branch length leads to a *sampled ancestor* while an internal edge with zero branch length is part of a *polytomy*.

Throughout this paper, we assume that the topology τ of the tree is known and we are interested in reconstructing the vector of branch lengths. We allow the individual branch length q_e to be zero, which enables us to consider non-bifurcating trees. Since the tree topology is fixed, the tree is completely represented by the vector of branch lengths q . We will consider the set \mathcal{T} of all phylogenetic trees with topology τ and branch lengths bounded from above by some $g_0 > 0$. This arbitrary upper bound on branch lengths is for mathematical convenience and does not represent a real constraint for the short-term evolutionary setting of interest here.

2.2. Phylogenetic likelihood. We will follow the most common setting for likelihood-based phylogenetics: a reversible continuous-time Markov chain model of substitution which is IID across sites. Briefly, let Ω denote the set of states and let $r = |\Omega|$; for convenience, we assume the states have indices 1 to r . We assume that mutation events occur according to a continuous time Markov chain on states Ω . Specifically, the probability of ending in state y after time t given that the site started in state x is given by the xy -th entry of $P(t)$, where $P(t)$ is the matrix valued function $P = e^{Qt}$, and the matrix Q is the instantaneous rate matrix of the evolutionary model. The branch length t of a given edge represents the time during which the mutation process operates. We assume that the rate matrix Q is reversible with respect to a stationary distribution π on the set of states Ω .

We will use the term *state assignment* to refer to a single-site labelling of the leaf of tree by characters in Ω . For a fixed vector of branch lengths q , the phylogenetic likelihood is defined as follows and will be denoted by $L(p)$. Let $\mathbf{Y}^k = (\mathbf{Y}^{(1)}, \mathbf{Y}^{(2)}, \dots, \mathbf{Y}^{(k)}) \in \Omega^{N \times k}$ be the observed sequences (with characters in Ω) of length k over N leaves (i.e., each of the $\mathbf{Y}^{(i)}$'s is a state assignment). The likelihood of observing \mathbf{Y} given the tree has the form

$$L_k(q) = \prod_{i=1}^k \sum_{a^i} \eta(a^i) \prod_{(u,v) \in E} P_{a_u^i a_v^i}(q_{uv})$$

where ρ is any internal node of the tree, a^i ranges over all extensions of $\mathbf{Y}^{(i)}$ to the internal nodes of the tree, a_u^i denotes the assigned state of node u by a^i , $P_{xy}(t)$ denotes the transition probability from character x to character y across an edge of length t defined by a given evolutionary model and η is the stationary distribution of this evolutionary model. The value of the likelihood does not depend on choice of ρ due to the reversibility assumption.

We will also denote $\ell_k(q) = \log(L_k(q))$ and refer to it as the log-likelihood function given the observed sequence. We allow the likelihood of a tree given data to be zero, and thus ℓ_k is defined on \mathcal{T} with values in the extended real line $[-\infty, 0]$. We note that ℓ_k is continuous, that is, for any vector of branch lengths $q_0 \in \mathcal{T}$, we have

$$\lim_{q \rightarrow q_0} \ell_k(q) = \ell_k(q_0)$$

even if $\ell_k(q_0) = -\infty$.

Each vector of branch lengths q generates a distribution on the state assignment of the leaves, hereafter denoted by P_q . We will make the following assumptions:

Assumption 2.1 (Model identifiability). $P_q = P_{q'} \Leftrightarrow q = q'$.

Assumption 2.2. *The data \mathbf{Y}^k are generated on a tree topology τ with vector of branch lengths $q^* \in \mathcal{T}$ according to the above Markov process, where some components of q^* might be zero. We assume further that the tree distance (the sum of branch lengths) between any pair of leaves of the true tree is strictly positive.*

The second criterion ensures that no two leaves will be labeled with identical sequences as sequence length k becomes long.

2.3. Regularized estimators for phylogenetic inference. Throughout the paper, we consider regularization-type estimators, which are defined as the minimizer of the phylogenetic likelihood function penalized with various R_k :

$$(2.1) \quad q^{k, R_k} = \operatorname{argmin}_{q \in \mathcal{T}} -\frac{1}{k} \ell_k(q) + \lambda_k R_k(q).$$

Here R_k denotes the penalty function and λ_k is the regularization parameter that controls how the penalty function impacts the estimates. Different forms of the penalty function will lead to different statistical estimators of the generating tree.

The existence of a minimizer as in (2.1) is guaranteed by the following Lemma (proof in Appendix):

Lemma 2.3. *If the penalty R_k is continuous on \mathcal{T} , then for $\lambda > 0$ and observed sequences \mathbf{Y}^k , there exists a $q \in \mathcal{T}$ minimizing*

$$Z_{\lambda, \mathbf{Y}^k}(q) = -\frac{1}{k} \ell_k(q) + \lambda R_k(q).$$

We are especially interested in the ability of the estimators to detect polytomies and sampled ancestors. This leads us the following definition of topological consistency, which in the usual variable selection setting is sometimes called *sparsistency*.

Definition 2.4. *For any vector of branch lengths q , we denote the index set of zero entries*

$$\mathcal{A}(q) = \{i : q_i = 0\}.$$

We say a regularized estimator with penalty function R_k is topologically consistent if for all data-generating branch lengths q^ , we have*

$$\lim_{k \rightarrow \infty} \mathbb{P}(\mathcal{A}(q^{k, R_k}) = \mathcal{A}(q^*)) = 1.$$

Definition 2.5 (Phylogenetic LASSO). *The phylogenetic LASSO estimator is (2.1) with the standard LASSO penalty $R_k^{[0]}$, which in our setting of non-negative q_i is*

$$R_k^{[0]}(q) = \lambda_k^{[0]} \sum_{i \in E} q_i.$$

We will use $q^{k, R_k^{[0]}}$ to denote the phylogenetic LASSO estimate, namely

$$q^{k, R_k^{[0]}} = \operatorname{argmin}_{q \in \mathcal{T}} -\frac{1}{k} \ell_k(q) + \lambda_k^{[0]} \sum_{i \in E} q_i.$$

Definition 2.6 (Adaptive LASSO (Zou, 2006)). *The phylogenetic adaptive LASSO estimator is (2.1) with penalty function*

$$R_k^{[1]}(q) = \lambda_k^{[1]} \sum_{i \in E} w_{k,i} q_i \quad \text{where} \quad w_{k,i} = \left(q_i^{k, R_k^{[0]}} \right)^{-\gamma}$$

for some $\gamma > 0$ and $q^{k, R_k^{[0]}}$ is the phylogenetic LASSO estimate.

Definition 2.7 (Multiple-step adaptive LASSO (Bühlmann and Meier, 2008)). *The phylogenetic multiple-step LASSO is defined recursively with the phylogenetic LASSO estimator as the base case ($m = 1$), and the penalty function in (2.1) at step m being*

$$R_k^{[m]}(q) = \lambda_k^{[m]} \sum_{i \in E} w_{k,i} q_i \quad \text{where} \quad w_{k,i} = \left(q_i^{k, R_k^{[m-1]}} \right)^{-\gamma},$$

where $\gamma > 0$ and $q^{k, R_k^{[m-1]}}$ is the $(m - 1)$ -step regularized estimator with penalty function $R_k^{[m-1]}(q)$.

3. THEORETICAL PROPERTIES OF LASSO-TYPE REGULARIZED ESTIMATORS FOR PHYLOGENETIC INFERENCE

We next show convergence and topological consistency of the LASSO-type phylogenetic estimates introduced in the previous section. As described in the introduction, phylogenetic LASSO is a non-convex regularization problem for which the true estimates lie on the boundary of a space on which the likelihood function is untamed. To circumvent those problems, we take a minor departure from the standard approach for analysis of non-convex regularization: instead of imposing regularity conditions directly on the empirical log-likelihood function, we investigate the expected per-site log likelihood and investigate its regularity. This function enables us to isolate the singular points and derive a local regularity condition that is similar to the Restricted Strong Convexity condition (Loh and Wainwright, 2013; Loh, 2017). This leads us to study the fast-rate generalization of the empirical log-likelihood in a PAC learning framework (Van Erven et al., 2015; Dinh et al., 2016).

3.1. Definitions and lemmas. We begin by setting the stage with needed definitions and lemmas. Most proofs are deferred to the Appendix.

Definition 3.1. *We define the expected per-site log-likelihood*

$$\phi(q) := \mathbb{E}_{\psi \sim P_{q^*}} [\log P_q(\psi)]$$

for any vector of branch lengths q .

Definition 3.2. *For any $\mu > 0$, we denote by $\mathcal{T}(\mu)$ the set of all branch length vectors $q \in \mathcal{T}$ such that $\log P_q(\psi) \geq -\mu$ for all state assignments ψ to the leaves.*

We have the following result, where $\|\cdot\|_2$ is the ℓ_2 -norm in \mathbb{R}^{2N-3} .

Lemma 3.3 (Limit likelihood). *The vector q^* is the unique maximizer of ϕ , and $\forall q \in \mathcal{T}$*

$$(3.1) \quad \frac{1}{k} \ell_k(q) \rightarrow \phi(q) \quad \text{a.s.}$$

Moreover, there exist $\beta \geq 2$ and $c_1 > 0$ depending on N, Q, η, g_0, μ such that

$$(3.2) \quad c_1^\beta \|q - q^*\|_2^\beta \leq |\phi(q) - \phi(q^*)| \quad \forall q \in \mathcal{T}(\mu).$$

Proof. The first statement follows from the identifiability assumption, and (3.1) is a direct consequence of the Law of Large Numbers. Equation 3.2 follows from the Lojasiewicz inequality (Ji et al., 1992) for ϕ on \mathcal{T} , which applies because ϕ is an analytic function defined on the compact set \mathcal{T} with q^* as its only maximizer in \mathcal{T} . \square

Group-based DNA sequence evolution models are a class of relatively simple models that have transition matrix structure compatible with an algebraic group (Evans and Speed, 1993). From Lemma 6.1 of Dinh et al. (2016), we have

Remark 3.4. For group-based models, $\beta = 2$.

For any $\mu > 0$, we also have the following estimates showing local Lipschitzness of the log-likelihood functions, recalling that k is the number of sites.

Lemma 3.5. For any $\mu > 0$, there exists a constant $c_2(N, Q, \eta, g_0, \mu) > 0$ such that

$$(3.3) \quad \left| \frac{1}{k} \ell_k(q) - \frac{1}{k} \ell_k(q') \right| \leq c_2 \|q - q'\|_2$$

and

$$(3.4) \quad |\phi(q) - \phi(q')| \leq c_2 \|q - q'\|_2$$

for all $q, q' \in \mathcal{T}(\mu)$.

Fix an arbitrary $\mu > 0$. For any $q \in \mathcal{T}(\mu)$ we consider the *excess loss*

$$U_k(q) = \frac{1}{k} \ell_k(q^*) - \frac{1}{k} \ell_k(q).$$

and derive a PAC lower bound on the deviation of the excess loss from its expected value on $\mathcal{T}(\mu)$. First note that since the sites \mathbf{Y}^k are independent and identically distributed, we have

$$\mathbb{E}[U_k(q)] = \mathbb{E} \left[\frac{1}{k} \ell_k(q^*) - \frac{1}{k} \ell_k(q) \right] = \phi(q^*) - \phi(q).$$

Moreover, from Lemma 3.5, we have $|U_k(q)| \leq c_2 \|q - q^*\|_2$. Applying this in the case $k = 1$ and noting that $U_k(q)$ is the average of k IID copies of $U_1(q)$, we have that $\text{Var}[U_k(q)] \leq c_2^2 \|q - q^*\|_2^2 / k$. This implies by (3.2) that

$$(3.5) \quad \text{Var}[U_k(q)] \leq \frac{c_2^2}{k} \|q - q^*\|_2^2 \leq \frac{c_2^2}{k c_1^2} \mathbb{E}[U_k(q)]^{2/\beta}$$

for all $q \in \mathcal{T}(\mu)$.

Lemma 3.6. Let G_k be the set of all branch length vectors $q \in \mathcal{T}(\mu)$ such that $\mathbb{E}[U_k(q)] \geq 1/k$. Let $\beta \geq 2$ be the constant in Lemma 3.3. For any $\delta > 0$ and previously specified variables there exists $C(\delta, N, Q, \eta, g_0, \mu, \beta) \geq 1$ (independent of k) such that for any $k \geq 3$, we have:

$$U_k(q) \geq \frac{1}{2} \mathbb{E}[U_k(q)] - \frac{C \log k}{k^{2/\beta}} \quad \forall q \in G_k$$

with probability greater than $1 - \delta$.

We also need the following preliminary lemma from (Dinh et al., 2016).

Lemma 3.7. *Given $0 < \nu < 1$, there exist constants $C_1, C_2 > 0$ depending only on ν such that for all $x > 0$, if $x \leq ax^\nu + b$ then $x \leq C_1 a^{1/(1-\nu)} + C_2 b$.*

3.2. Convergence and topological consistency of regularized phylogenetics. We now show convergence and topological consistency of q^{k, R_k} , the regularized estimator (2.1) for various choices of penalty R_k as the sequence length k increases. For convenience, we will assume throughout this section that the parameters N, Q, η, g_0, μ and β (defined in the previous section) are fixed.

3.2.1. Convergence. We first have the following two lemmas guaranteeing that if μ is carefully chosen, a neighborhood V of q^* and the regularized estimator q^{k, R_k} lie inside $\mathcal{T}(\mu)$ with high probability.

Lemma 3.8. *There exist $\mu^* > 0$ and an open neighborhood V of q^* in \mathcal{T} such that $V \subset \mathcal{T}(\mu^*)$.*

Lemma 3.9. *If the sequence $\{\lambda_k R_k(q^*)\}$ is bounded, then for any $\delta > 0$, there exist $\mu(\delta) > 0$ and $K(\delta) > 0$ such that for all $k \geq K$, $q^{k, R_k} \in \mathcal{T}(\mu)$ with probability at least $1 - 2\delta$.*

We are now ready to prove a series of theorems establishing consistency and topological consistency of phylogenetic adaptive and multi-step adaptive LASSO. As part of this development we will first use as a hypothesis and then establish the technical condition that there exists a $C_3 > 0$ independent of k such that

$$(3.6) \quad |R_k(q^{k, R_k}) - R_k(q^*)| \leq C_3 \|q^{k, R_k} - q^*\|_2 \quad \forall k.$$

This will form an essential part of our recursive proof. As the first step in this project, choosing μ to satisfy these lemmas, we can use the deviation bound of Lemma 3.6 to prove

Theorem 3.10. *If $\lambda_k R_k(q^*) \rightarrow 0$ then $\{q^{k, R_k}\}$ converges to q^* almost surely.*

Moreover, letting $\beta \geq 2$ be the constant in Lemma 3.3, for any $\delta > 0$ there exist $C(\delta) > 0$ and $K(\delta) > 0$ such that for all $k \geq K$, with probability at least $1 - \delta$ we have

$$(3.7) \quad \|q^{k, R_k} - q^*\|_2 \leq C(\delta) \left(\frac{\log k}{k^{2/\beta}} + \lambda_k R_k(q^*) \right)^{1/\beta}.$$

If we assume further that there exists a $C_3 > 0$ independent of k satisfying (3.6) then there exists $C'(\delta) > 0$ such that for all $k \geq K$,

$$\|q^{k, R_k} - q^*\|_2 \leq C'(\delta) \left(\frac{\log k}{k^{2/\beta}} + \lambda_k^{\beta/(\beta-1)} \right)^{1/\beta}$$

with probability at least $1 - \delta$.

Proof. By definition of the estimator, we have

$$-\frac{1}{k} \ell_k(q^{k, R_k}) + \lambda_k R_k(q^{k, R_k}) \leq -\frac{1}{k} \ell_k(q^*) + \lambda_k R_k(q^*)$$

which is equivalent to $U_k(q^{k, R_k}) \leq \lambda_k R_k(q^*) - \lambda_k R_k(q^{k, R_k})$.

We have $q^{k,R_k} \in \mathcal{T}(\mu)$ with probability at least $1 - 2\delta$ from Lemma 3.9 for k sufficiently large. Therefore by Lemma 3.6,

$$\mathbb{E}[U_k(q^{k,R_k})] \leq \frac{1}{k} \quad \text{or} \quad \frac{1}{2}\mathbb{E}[U_k(q^{k,R_k})] \leq U_k(q^{k,R_k}) + \frac{C \log k}{k^{2/\beta}},$$

with probability at least $1 - 3\delta$. The second case implies that

$$\begin{aligned} \frac{c_1^\beta}{2} \|q^{k,R_k} - q^*\|_2^\beta &\leq \frac{1}{2}\mathbb{E}[U_k(q^{k,R_k})] \\ &\leq \lambda_k R_k(q^*) - \lambda_k R_k(q^{k,R_k}) + \frac{C \log k}{k^{2/\beta}} \leq \frac{C \log k}{k^{2/\beta}} + \lambda_k R_k(q^*) \end{aligned}$$

while for the first case, we have

$$\frac{c_1^\beta}{2} \|q^{k,R_k} - q^*\|_2^\beta \leq \mathbb{E}[U_k(q^{k,R_k})] \leq \frac{1}{k} \leq \frac{C \log k}{k^{2/\beta}} + \lambda_k R_k(q^*).$$

since $\beta \geq 2$ and $C \geq 1$. This demonstrates (3.7).

If the additional assumption (3.6) is satisfied, we also have

$$\|q^{k,R_k} - q^*\|_2^\beta \leq \frac{C' \log k}{k^{2/\beta}} + C_3 \lambda_k \|q^{k,R_k} - q^*\|_2.$$

Using Lemma 3.7 with

$$\nu = 1/\beta, \quad x = \|q^{k,R_k} - q^*\|_2^\beta, \quad a = C_3 \lambda_k \quad \text{and} \quad b = \frac{C' \log k}{k^{2/\beta}},$$

we obtain

$$x \leq C_1 a^{1/(1-\nu)} + C_2 b,$$

which implies

$$\|q^{k,R_k} - q^*\|_2^\beta \leq C'(\delta, C_3) \left(\frac{\log k}{k^{2/\beta}} + \lambda_k^{\beta/(\beta-1)} \right).$$

This completes the proof. \square

3.2.2. Topological consistency. The goal of this section is to prove that the phylogenetic LASSO is able to detect zero edges, which then give polytomies and sampled ancestors. Since the estimators are defined recursively, we will establish these properties of adaptive and multi-step phylogenetic LASSO through an inductive argument. Throughout this section, we will continue to use q^{k,R_k} to denote the regularized estimator (2.1). We will use q^{k,S_k} to denote the corresponding adaptive estimator where $S_k(q) = \sum_i w_{k,i} q_i$ and $w_{k,i} = \left(q_i^{k,R_k}\right)^{-\gamma}$ for some $\gamma > 0$. We will use α_k to be the regularizing parameter for the second step (regularizing with S_k) and keep λ_k as the parameter for the first step. These two need not be equal.

For positive sequences f_k, g_k , we will use the notation $f_k \succ g_k$ to mean that $\lim_{k \rightarrow \infty} f_k/g_k = \infty$. We have the following result showing consistency of adaptive LASSO, and setting the stage to show topological consistency of adaptive LASSO.

Theorem 3.11. *Assume that $\lambda_k \rightarrow 0$, $R_k(q^*) = \mathcal{O}(1)$ and that*

$$\alpha_k \rightarrow 0, \quad \alpha_k \succ \left(\frac{\log k}{k^{2/\beta}} \right)^{\gamma/\beta}, \quad \alpha_k \succ \lambda_k^{\gamma/(\beta-1)}.$$

We have

- (i) $S_k(q^*) = \mathcal{O}(1)$ and the estimator q_k^S is consistent.

(ii) *If there exists C_3 independent of k satisfying (3.6) then the estimator q_k^S is topologically consistent.*

Proof. We first note that by Theorem 3.10, the estimator q^{k,R_k} is consistent, which guarantees $\lim_{k \rightarrow \infty} q^{k,R_k} = q^*$ almost surely. Thus

$$\lim_{k \rightarrow \infty} S_k(q^*) = \lim_{k \rightarrow \infty} \sum_{q_i^* \neq 0} (q_i^*)^{1-\gamma} < \infty.$$

The hypotheses of this theorem imply that $\lambda_k \rightarrow 0$ and thus by Theorem 3.10, we also deduce that q^{k,S_k} is also a consistent estimator. This validates (i).

To establish topological consistency under (ii), we divide the proof into two steps.

As the first step, we prove that $\lim_k \mathbb{P}(\mathcal{A}(q^*) \subset \mathcal{A}(q^{k,S_k})) = 1$. If $q_{i_0}^* = 0$ for some i_0 , then from Theorem 3.10, we have

$$q_{i_0}^{k,R_k} \leq C'(\delta) \left(\frac{\log k}{k^{2/\beta}} + \lambda_k^{\beta/(\beta-1)} \right)^{1/\beta} \quad \forall k$$

with probability at least $1 - \delta$. By the definition of w_{k,i_0} , we have

$$\begin{aligned} \lim_{k \rightarrow \infty} \alpha_k w_{k,i_0} &\geq \lim_{k \rightarrow \infty} \alpha_k (C'(\delta))^{-\gamma} \left(\frac{\log k}{k^{2/\beta}} + \lambda_k^{\beta/(\beta-1)} \right)^{-\gamma/\beta} \\ &= (C'(\delta))^{-\gamma} \lim_{k \rightarrow \infty} \left(\frac{\log k}{\alpha_k^{\beta/\gamma} k^{2/\beta}} + \alpha_k^{-\beta/\gamma} \lambda_k^{\beta/(\beta-1)} \right)^{-\gamma/\beta} \end{aligned}$$

which goes to infinity since by the hypotheses of the Theorem

$$\alpha_k^{\beta/\gamma} \succ \frac{\log k}{k^{2/\beta}} \quad \text{and} \quad \alpha_k^{\beta/\gamma} \succ \lambda_k^{\beta/(\beta-1)}.$$

Since $\delta > 0$ is arbitrary, we deduce that $\lim_{k \rightarrow \infty} \alpha_k w_{k,i_0} = \infty$ with probability one.

Now for any branch length vector q , we define $f(q)$ as the vector obtained from q by setting the i_0 component of q to 0. By definition of the estimator q^{k,S_k} , we have

$$-\frac{1}{k} \ell_k(q^{k,S_k}) + \alpha_k \sum_i w_{k,i} q_i^{k,S_k} \leq -\frac{1}{k} \ell_k(f(q^{k,S_k})) + \alpha_k \sum_i w_{k,i} [f(q^{k,S_k})]_i$$

or equivalently

$$\alpha_k w_{k,i_0} q_{i_0}^{k,S_k} \leq \frac{1}{k} \ell_k(q^{k,S_k}) - \frac{1}{k} \ell_k(f(q^{k,S_k})).$$

Lemma 3.8 establishes that there exist, $\mu^* > 0$ and a neighborhood V of q^* in \mathcal{T} such that $V \subset \mathcal{T}(\mu^*)$. Since the estimator q^{k,S_k} is consistent and $q_{i_0}^* = 0$, we can assume that both q^{k,S_k} and $f(q^{k,S_k})$ belong to $\mathcal{T}(\mu^*)$ with k large enough. Thus, from Lemma 3.5, we have

$$\left| \frac{1}{k} \ell_k(q^{k,S_k}) - \frac{1}{k} \ell_k(f(q^{k,S_k})) \right| \leq c_2 \|q^{k,S_k} - f(q^{k,S_k})\|_2 = c_2 q_{i_0}^{k,S_k}.$$

If $q_{i_0}^{k,S_k} > 0$, we deduce that $\alpha_k w_{k,i_0}$ is bounded from above by c_2 , which is a contradiction. This implies that $q_{i_0}^{k,S_k} = 0$, and we conclude that

$$\lim_k \mathbb{P}(\mathcal{A}(q^*) \subset \mathcal{A}(q^{k,S_k})) = 1.$$

As the second step, we prove that $\lim_k \mathbb{P}(\mathcal{A}(q^{k,S_k}) \subset \mathcal{A}(q^*)) = 1$. Indeed, the consistency of q^{k,S_k} guarantees that

$$\lim_{k \rightarrow \infty} q^{k,S_k} = q^*.$$

almost surely. Therefore, if $q_{i_0}^* > 0$ for some i_0 , then $q_{i_0}^{k,S_k} > 0$ for k large enough. In other words, we have $\lim_k \mathbb{P}(\mathcal{A}(q^{k,S_k}) \subset \mathcal{A}(q^*)) = 1$.

Combing step 1 and step 2, we deduce that the adaptive estimator is topologically consistent. \square

Lemma 3.12. *If q^{k,S_k} is topologically consistent and q^{k,R_k} is consistent, then there exists a C_3 independent of k such that*

$$|S_k(q^{k,S_k}) - S_k(q^*)| \leq C_3 \|q^{k,S_k} - q^*\|_2 \quad \forall k.$$

Proof. Since q^{k,S_k} is topologically consistent and q^{k,R_k} is consistent, we have

$$\mathcal{A}(q^{k,S_k}) = \mathcal{A}(q^*) \quad \text{and} \quad q_i^{k,R_k} \geq q_i^*/2 \quad \forall i \notin \mathcal{A}(q^*)$$

with probability one for sufficiently large k . Defining $b = \min_{i \notin \mathcal{A}(q^*)} q_i^*$, we have

$$|S_k(q^{k,S_k}) - S_k(q^*)| = \left| \sum_{q_i^* \neq 0} w_{k,i} (q_i^{k,S_k} - q_i^*) \right| \leq \sqrt{2N-3} (b/2)^{-\gamma} \|q^{k,S_k} - q^*\|_2$$

via Cauchy-Schwarz which completes the proof. \square

Theorem 3.13. *If*

$$\lambda_k^{[m]} \rightarrow 0, \quad \lambda_k^{[m]} \succ \left(\frac{\log k}{k^{2/\beta}} \right)^{\gamma/\beta}, \quad \forall m = 0, \dots, M$$

and

$$(3.8) \quad \lambda_k^{[m]} \succ \left(\lambda_k^{[m-1]} \right)^{\gamma/(\beta-1)} \quad \forall m = 1, \dots, M$$

then

- (i) *The adaptive LASSO and the m -step LASSO are topologically consistent for all $1 \leq m \leq M$.*
- (ii) *For all $0 \leq m \leq M$, the m -step LASSO (including the phylogenetic LASSO and adaptive LASSO) are consistent. Moreover, for all $\delta > 0$ and $0 \leq m \leq M$, there exists $C^{[m]}(\delta) > 0$ such that for all $k \geq K$,*

$$\|q^{k,R_k^{[m]}} - q^*\|_2 \leq C^{[m]}(\delta) \left(\frac{\log k}{k^{2/\beta}} + \left(\lambda_k^{[m]} \right)^{\beta/(\beta-1)} \right)^{1/\beta}$$

with probability at least $1 - \delta$. In other words, the convergence of m -step LASSO is of order

$$\mathcal{O}_P \left(\left(\frac{\log k}{k^{2/\beta}} + \left(\lambda_k^{[m]} \right)^{\beta/(\beta-1)} \right)^{1/\beta} \right)$$

where \mathcal{O}_P denotes big- O -in-probability.

Proof. We note that for the LASSO estimator, $R_k^{[0]}(q^*) = \sum_i q_i^*$ is uniformly bounded from above. Hence, the LASSO estimator is consistent. We can then use this as the base case to prove, by induction, that adaptive LASSO and the multiple-step LASSO are consistent via Theorem 3.11 (part (i)). Moreover, $R_k^{[0]}$ is uniformly Lipschitz and satisfies (3.6), so using part (ii) of Theorem 3.11, we deduce that adaptive LASSO (i.e., the estimator with penalty function $R_k^{[1]}$) is topologically consistent.

We will prove that the multiple-step LASSOs are topologically consistent by induction. Assume that $q^{k, R_k^{[m]}}$ is topologically consistent, and that $q^{k, R_k^{[m-1]}}$ is consistent. From Lemma 3.12, we deduce that there exists $C > 0$ independent of k such that

$$(3.9) \quad \left| R_k^{[m]} \left(q^{k, R_k^{[m]}} \right) - R_k^{[m]}(q^*) \right| \leq C \left\| q^{k, R_k^{[m]}} - q^* \right\|_2 \quad \forall k.$$

This enables us to use part (ii) of Theorem 3.11 to conclude that $q^{k, R_k^{[m+1]}}$ is topologically consistent. This inductive argument proves part (i) of the Theorem. We can now use (3.9) and Theorem 3.10 to derive the convergence rate of the estimators. \square

Remark 3.14. *If we further assume that $\gamma > \beta - 1$, then the results of Theorem 3.13 are valid if $\lambda_k^{[m]}$ is independent of m . This enables us to keep the regularizing parameters λ_k unchanged through successive applications of the multi-step estimator.*

Similarly, the Theorem applies if $\gamma > \beta - 1$ and

$$\lambda_k^{[m]} / \lambda_k^{[m-1]} \rightarrow c^{[m]} > 0$$

for all $m = 1, \dots, M$.

Remark 3.15. *Consider the case $\beta = 2$ (for example, for group-based models), $\epsilon > 0$ and $\gamma > 1$. If we choose $\lambda_k^{[m]} = \lambda_k$ (independent of m) such that*

$$\lambda_k \sim \frac{(\log k)^{1/2+\epsilon}}{\sqrt{k}},$$

then the convergence of m -step LASSO is of order

$$\mathcal{O}_P \left(\frac{(\log k)^{1/2+\epsilon}}{\sqrt{k}} \right).$$

4. ALGORITHMS

In this section, we aim to design a robust solver for the phylogenetic LASSO problem. Many efficient algorithms have been proposed for the LASSO minimization problem

$$(4.1) \quad \hat{q} = \arg \min_q g(q) + \lambda \|q\|_1$$

for a variety of objective functions g . When $g(q) = \|Y - Xq\|_2^2$, Efron et al. (2004) introduced *least angle regression* (LARS) that computes not only the estimates but also the solution path efficiently. In more general settings, *iterative shrinkage-thresholding algorithm* (ISTA) is a typical proximal gradient method that utilizes an efficient and sparsity-promoting proximal mapping operator (also known as soft-thresholding operator) in each iteration. Adopting Nesterov's acceleration

technique, Beck and Teboulle (2009) proposed a fast ISTA (FISTA) that has been proved to significantly improve the convergence rate.

These previous algorithms do not directly apply to phylogenetic LASSO. LARS is mainly designed for regression and does not apply here. Classical proximal gradient methods are not directly applicable for the phylogenetic LASSO for the following reasons: (i) *Nonconvexity*. The negative log phylogenetic likelihood is usually non-convex. Therefore, the convergence analysis (which is described briefly in the following section 4.1) may not hold. Moreover, nonconvexity also makes it much harder to adapt to local smoothness which could lead to slow convergence. (ii) *Bounded domain*. ISTA and FISTA also assume there are no constraints while in phylogenetic inference we need the branches to be nonnegative: $q \geq 0$. (iii) *Regions of infinite cost*. Unlike normal cost functions, the negative phylogenetic log-likelihood can be infinite especially when q is sparse as shown in the following proposition.

Proposition 4.1. *Let $\mathbf{Y} = (y_1, y_2, \dots, y_N) \in \Omega^N$ be an observed character vector on one site. If $y_i \neq y_j$ and there is a path $(u_0, u_1), (u_1, u_2), \dots, (u_s, u_{s+1})$, $u_0 = i, u_{s+1} = j$ on the topology τ such that $q_{u_k u_{k+1}} = 0$, $k = 0, \dots, s$, then*

$$L(\mathbf{Y}|q) = 0.$$

Proof. Let a be any extension of \mathbf{Y} to the internal nodes. Since $a_{u_0} = y_i \neq y_j = a_{u_{s+1}}$, there must be some $0 \leq k \leq s$ such that $a_{u_k} \neq a_{u_{k+1}} \Rightarrow P_{a_{u_k} a_{u_{k+1}}}(q_{u_k u_{k+1}}) = 0$. Therefore,

$$L(\mathbf{Y}|q) = \sum_a \eta(a_\rho) \prod_{(u,v) \in E} P_{a_u a_v}(q_{uv}) = 0.$$

□

In what follows, we briefly review the proximal gradient methods (ISTA) and their accelerations (FISTA), and provide an extension of FISTA to accommodate the above issues.

4.1. Proximal Gradient Methods. Consider the nonsmooth ℓ_1 regularized problem (4.1). Gradient descent generally does not work due to non-differentiability of the ℓ_1 norm. The key insight of the proximal gradient method is to view the gradient descent update as a minimization of a local linear approximation to g plus a quadratic term. This suggests the following update strategy

$$\begin{aligned} q^{(n+1)} &= \arg \min_q \left\{ g(q^{(n)}) + \langle \nabla g(q^{(n)}), q - q^{(n)} \rangle + \frac{1}{2t_n} \|q - q^{(n)}\|_2^2 + \lambda \|q\|_1 \right\} \\ (4.2) \quad &= \arg \min_q \left\{ \frac{1}{2t_n} \left\| q - \left(q^{(n)} - t_n \nabla g(q^{(n)}) \right) \right\|_2^2 + \lambda \|q\|_1 \right\} \end{aligned}$$

where (4.2) corresponds to the proximal map of $h(q) = \|q\|_1$, which is defined as follows

$$(4.3) \quad \mathbf{prox}_{th}(p) := \arg \min_q \left\{ \frac{1}{2} \|q - p\|_2^2 + th(q) \right\} = \arg \min_q \left\{ \frac{1}{2t} \|q - p\|_2^2 + h(q) \right\}$$

(4.3) is usually easy to solve if the regularization function h is simple. For example, in case of $h(q) = \|q\|_1$, it can be solved by the *soft thresholding operator*

$$\mathcal{S}_t(p) = \text{sign}(p)(|p| - t)_+$$

where $x_+ = \max\{x, 0\}$. Applying this operator to (4.2), we get the ISTA update formula

$$(4.4) \quad q^{(n+1)} = \mathcal{S}_{\lambda t_n}(q^{(n)} - t_n \nabla g(q^{(n)})).$$

Let $f = g + \lambda \|q\|_1$. Assume g is convex and ∇g is Lipschitz continuous with Lipschitz constant $L_{\nabla g} > 0$; if a constant step size is used and $t_n = t < 1/L_{\nabla g}$, then ISTA converges at rate

$$(4.5) \quad f(q^{(n)}) - f(q^*) \leq \frac{1}{2tn} \|q^{(0)} - q^*\|_2^2$$

where q^* is the optimal solution. This means ISTA has *sublinear convergence* whenever the stepsize is in the interval $(0, 1/L_{\nabla g}]$. Note that ISTA could have linear convergence if g is strongly convex.

The convergence rate in (4.5) can be significantly improved using Nesterov's acceleration technique. The acceleration comes from a weighted combination of the current and previous gradient directions, which is similar to gradient descent with momentum. This leads to Algorithm 1 which is essentially equivalent to the *fast iterative shrinkage-thresholding algorithm* (FISTA) introduced by Beck and Teboulle (2009). Under the same condition, FISTA enjoys a significantly faster convergence rate

$$(4.6) \quad f(q^{(n)}) - f(q^*) \leq \frac{2}{t(n+1)^2} \|q^{(0)} - q^*\|_2^2.$$

Notice that the above convergence rates both require the stepsize $t \leq 1/L_{\nabla g}$. In practice, however, the Lipschitz coefficient $L_{\nabla g}$ is usually unavailable and *back-tracking line search* is commonly used.

Algorithm 1 Fast Iterative Shrinkage-Thresholding Algorithm (FISTA)

Input: $q^{(0)}, t, \lambda$

1: Set $q^{(-1)} = q^{(0)}, n = 1$

2: **while** not converged **do**

3: $p \leftarrow q^{(n-1)} + \frac{n-2}{n+1}(q^{(n-1)} - q^{(n-2)})$ ▷ Nesterov's Acceleration

4: $q^{(n)} \leftarrow \mathcal{S}_{\lambda t}(p - t \nabla g(p))$ ▷ Soft-Thresholding Operator

5: $n \leftarrow n + 1$

6: **end while**

Output: $q^* \leftarrow q^{(n)}$

4.2. Projected FISTA. FISTA usually assumes no constraints for the parameters. However, in the phylogenetic case branch lengths are must be non-negative ($q \geq 0$). To address this issue, we combine the projected gradient method (which can be viewed as proximal gradient as well) with FISTA to assure non-negative updates. We refer to this hybrid as *projected FISTA* (pFISTA). Note that a similar strategy has been adopted by Liu et al. (2016) in tight frames based magnetic resonance image reconstruction. Let \mathcal{C} be a convex feasible set, define the indicator function $I_{\mathcal{C}}$ of the set \mathcal{C} :

$$I_{\mathcal{C}}(q) = \begin{cases} 0 & \text{if } q \in \mathcal{C}, \text{ and} \\ +\infty & \text{otherwise} \end{cases}$$

With the constraint $q \in \mathcal{C}$, we consider the following projected proximal gradient update

$$\begin{aligned}
 q^{(n+1)} &= \arg \min_{q \in \mathcal{C}} \left\{ g(p) + \langle \nabla g(p), q - p \rangle + \frac{1}{2t_n} \|q - p\|_2^2 + h(q) \right\} \\
 &= \arg \min_q \left\{ g(p) + \langle \nabla g(p), q - p \rangle + \frac{1}{2t_n} \|q - p\|_2^2 + h(q) + I_{\mathcal{C}}(q) \right\} \\
 (4.7) \quad &= \mathbf{prox}_{t_n h_{\mathcal{C}}}(p - t_n \nabla g(p))
 \end{aligned}$$

where $h_{\mathcal{C}} = h(q) + I_{\mathcal{C}}(q)$. Using *forward-backward splitting* (see Combettes and Wajs, 2006), (4.7) can be approximated as

$$(4.8) \quad \mathbf{prox}_{t_n h_{\mathcal{C}}}(p - t_n \nabla g(p)) \approx \Pi_{\mathcal{C}}(\mathbf{prox}_{t_n h}(p - t_n \nabla g(p)))$$

where $\Pi_{\mathcal{C}}$ is the Euclidean projection on to \mathcal{C} . When $h(q) = \|q\|_1$, $\mathcal{C} = \{q : q \geq 0\}$, we have the following pFISTA update formula

$$p = q^{(n)} + \frac{n-1}{n+2} (q^{(n)} - q^{(n-1)}), \quad q^{(n+1)} = [S_{\lambda t_n}(p_+ - t_n \nabla g(p_+))]_+.$$

Note that in this case, (4.8) is actually exact. Similarly, we can easily derive the projected ISTA (pISTA) update formula and we omit it here.

4.3. Restarting. To accommodate non-convexity and possible infinities of the phylogenetic cost function, we adopt the restarting technique introduced by O’Donoghue and Candes (2013) where they used it as a heuristic means of improving the convergence rate of accelerated gradient schemes. In the phylogenetic case, due to the non-convexity of negative phylogenetic log-likelihood, backtracking line search would fail to adapt to local smoothness which could lead to inefficient small step size. Moreover, the LASSO penalty will frequently push us into the “forbidden” zone $\{q : g(q) = +\infty\}$, especially when there are a lot of short branches. We therefore adjust the restarting criteria as follows:

- Small stepsize: restart whenever $t_n < \epsilon$.
- Infinite cost: restart whenever $g(p_+) = +\infty$.

Equipping FISTA with projection and adaptive restarting, we obtain an efficient phylogenetic LASSO solver that we summarize in Algorithm 2.

Algorithm 2 Projected FISTA with Restarting

Input: $q^{(0)}, t, \lambda, \epsilon, \omega \in (0, 1)$

- 1: **while** not converged **do**
- 2: Set $q^{(-1)} = q^{(0)}, t_1 = t, n = 1$
- 3: **while** not converged **do**
- 4: $p \leftarrow q^{(n-1)} + \frac{n-2}{n+1}(q^{(n-1)} - q^{(n-2)})$ \triangleright Nesterov's Acceleration
- 5: **if** $g(p_+) = +\infty$ **then** \triangleright Restarting
- 6: **break**
- 7: **end if**
- 8: $t_n \leftarrow t_{n-1}$
- 9: Adapt t_n through *backtracking line search* with ω
- 10: **if** $t_n < \epsilon$ **then** \triangleright Restarting
- 11: **break**
- 12: **end if**
- 13: $q^{(n)} \leftarrow [\mathcal{S}_{\lambda t_n}(p_+ - t_n \nabla g(p_+))]_+$ \triangleright Projected Soft-Thresholding

Operator

- 14: $n \leftarrow n + 1$
- 15: **end while**
- 16: Set $q^{(0)} = q^{(n-1)}$
- 17: **end while**

Output: $q^* \leftarrow q^{(n)}$

Remark 4.2. Note that the adaptive phylogenetic LASSO

$$(4.9) \quad \hat{q}^S = \arg \min_q g(q) + \lambda \sum_j w_j q_j$$

is equivalent to (using $/$ to denote componentwise division)

$$\tilde{q}^S = \arg \min_q \{g(q/w) + \lambda \|q\|_1\}, \quad \hat{q}^S = \tilde{q}^S / w.$$

Therefore, Algorithm 2 can also be used to solve the (multi-step) adaptive phylogenetic LASSO.

5. EXPERIMENTS

In this section, we first demonstrate the efficiency of the proposed algorithm for solving the phylogenetic LASSO problem when combined with maximum-likelihood phylogenetic inference. We then show (non-adaptive) phylogenetic LASSO does not appear to be strong enough to find zero edges on simulated data; adaptive phylogenetic LASSO performs much better. We then compare it with simple thresholding and rjMCMC then apply it to some real data sets. For all simulation and inference, we use the simplest Jukes and Cantor (1969) model of DNA substitution, in which all substitutions have equal rates. The code is made available at <https://github.com/matsengrp/adaLASSO-phylo>.

5.1. Efficiency of pFISTA for solving the phylogenetic LASSO. The fast convergence rate of FISTA (or pFISTA) need not hold when the cost function g is nonconvex. However, we can expect that g is well approximated by a quadratic

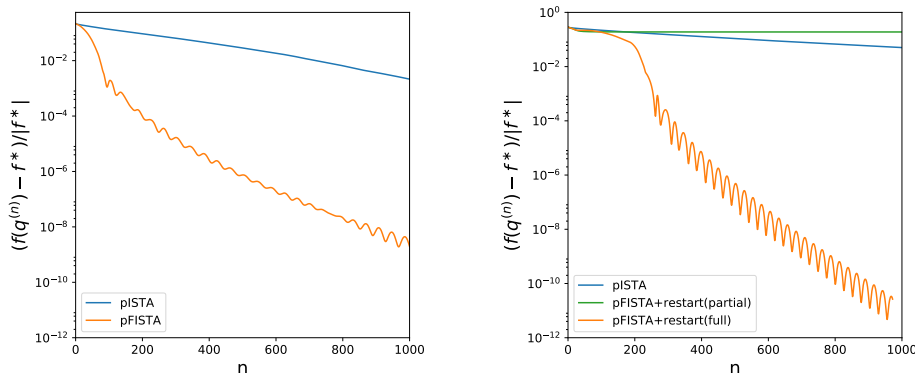


FIGURE 2. pISTA vs pFISTA on simulated data sets in terms of the relative error $(f(q^{(n)}) - f^*)/f^*$, each run with penalty coefficient $\lambda = 1.0$. Left panel: simulation 1; Right panel: simulation 2. In simulation 2, we tried two restarting strategies: restart whenever $g(p_+) = +\infty$ (partial) and restart whenever $t_n < \epsilon$ or $g(p_+) = +\infty$ (full). The optimal solution q^* is obtained from a long run of pFISTA.

function near the optimal (or some local mode) q^* . That is, there exists a neighborhood of q^* inside of which

$$g(q) \approx g(q^*) + \frac{1}{2}(q - q^*)^T \nabla^2 g(q^*)(q - q^*)$$

When we are eventually inside this domain, we will observe behavior consistent with the convergence analysis in Section 4.1.

To test the efficiency of pFISTA in different scenarios, we consider various simulated data sets generated from “sparse” unrooted trees with 100 tips and 50 randomly chosen zero branches as follows. All simulated data sets contain 1000 independent observations on the leaf nodes. We set the minimum step size $\epsilon = 5e-08$ for restarting.

We use the following simulation setups, in which branch lengths are expressed in the traditional units of expected number of substitutions per site.

Simulation 1. (*No short branches*). All nonzero branches have length 0.05. Because there are no short nonzero branches, branches that are originally nonzero are less likely to be collapsed to zero and we expect no restarting is needed.

Simulation 2. (*A few short branches*). For all the nonzero branches, we randomly choose 15 of them and set their lengths 0.002. All the other branches have length 0.05. In this setting, there are a few short branches that are likely to be shrunk to zero. As a result, several restarts may be needed before convergence.

We see that when the model does not have very short non-zero branches and the phylogenetic cost is more regular, pFISTA (and pISTA) finds the quadratic domain quickly and performs consistently with the corresponding convergence rate, even without restarting (Figure 2). When the model does have many very short branches and the negative phylogenetic log-likelihood is highly nonconvex, pFISTA

with restart still manages to arrive at the quadratic domain quickly and exhibits fast convergence thereafter. Furthermore, we find the *small stepsize* restarting criterion is useful to adapt to changing local smoothness and facilitate mode exploration. In both situations, pFISTA performs consistently better than pISTA. As a matter of fact, pISTA is monotonic so is more likely to get stuck in local minima, and hence may not be suitable for nonconvex optimization. We, therefore, use pFISTA with restart as our default algorithm in all the following experiments.

Remark 5.1. *Like other non-convex optimization algorithms, pFISTA with restart may be sensitive to the starting position of the parameters. However, due to the momentum introduced in Nesterov’s acceleration (which causes the ripples in Figure 2) and adaptive restarting, pFISTA with restart is more likely to escape local minima and potentially arrive at the global minimum.*

5.2. Performance of phylogenetic LASSO. Through simulation we also find that in practice the (non-adaptive) phylogenetic LASSO penalty is not strong enough to find all zero branches. Indeed, we find that phylogenetic LASSO only recovers around 60% of the sparsity found in the true models and larger penalty does not necessarily give more sparsity (Table 1). This suggests we use the adaptive phylogenetic LASSO that has been proven topologically consistent under mild conditions.

λ	1	5	10	20	40	80	160
Simulation 1	32	32	32	32	32	32	32
Simulation 2	32	32	32	32	32	32	31

TABLE 1. Number of zero length branches found for different penalty coefficients in both simulation models, each of which have 50 zero length branches.

5.3. Performance of adaptive phylogenetic LASSO. Next, we demonstrate that the topologically consistent (multistep) adaptive phylogenetic LASSO significantly enhances sparsity on simulated data compared to phylogenetic LASSO. We will use the more difficult simulation 2 that have a combination of zero and very short branches. In what follows (and for the rest of this section), we compute adaptive and multistep adaptive phylogenetic LASSO as described in Section 2.3. Note that $m = 1$ (first cycle) is the phylogenetic LASSO and $m = 2$ (second cycle) corresponds to the adaptive phylogenetic LASSO. Therefore, we can compare all phylogenetic LASSO estimators by simply running the multistep adaptive phylogenetic LASSO with the maximum cycle number $M \geq 2$. Since large γ often leads to severe adaptive weights and hence numerical instability, we use $\gamma = 1$ in the following experiments and put some results for $\gamma > 1$ (with guaranteed topological consistency) in the Appendix.

We run the multistep phylogenetic LASSO with $M = 4$ cycles. To test the topological consistency of the estimators, we use different initial regularization coefficients $\lambda^{[0]} = 10, 20, 30, 40, 50$ and update the regularization coefficients according

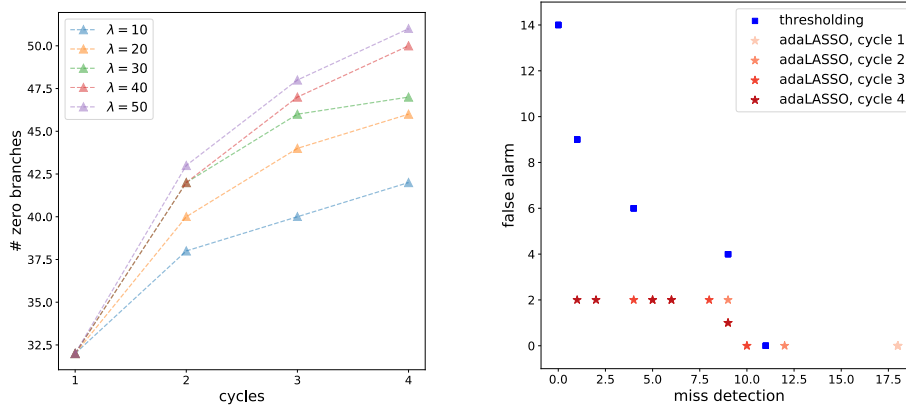


FIGURE 3. Topological consistency comparison of different phylogenetic LASSO procedures on simulation 2. Left panel: number of identified zero branches at different cycles (which corresponds to different phylogenetic LASSO procedures as aforementioned). Right panel: the number of misidentified zero branches (false alarm) and the number of unidentified zero branches (miss detection) for simple thresholding and multistep adaptive phylogenetic LASSO at different cycles.

to the following formula

$$\lambda^{[m]} = \lambda^{[m-1]} \frac{\text{mean}((\hat{q}^{[m]})^\gamma)}{\text{mean}((\hat{q}^{[m-1]})^\gamma)}$$

which maintains a relatively stable regularization among the adaptive LASSO steps. This formula provides reasonably good balance between sparsity and numerical stability in our experiments.

We find that multistep adaptive phylogenetic LASSO does improve sparsity identification while maintaining a relatively low misidentification rate. Indeed, as the cycle number increases, the estimator now is able to identify more zero branches (Figure 3, left panel). Moreover, unlike the phylogenetic LASSO ($m = 1$), we do observe more sparsity (identified zero branches) when the regularization coefficient increases at cycles $m > 1$. As more cycles are run and larger penalty coefficients are used, we see that multistep adaptive LASSO manages to reduce miss detection without introducing many extra false alarms (Figure 3, right panel). In contrast, simple thresholding is more likely to misidentify zero branches when larger thresholds are used to bring down miss detection.

5.4. Short Edge Detection. Previous work has proposed Bayesian approaches to infer non-bifurcating tree topologies by assigning priors that cover all of the tree space, including less-resolved (unresolved) tree topologies (Lewis et al., 2005, 2015). Since the numbers of branches (parameters) are different among those tree topologies, reversible-jump MCMC (rjMCMC) is commonly used. Both approaches provide means of sparsity encouragement that allow us to discover non-bifurcating tree topologies, which as described in the Introduction make different evolutionary

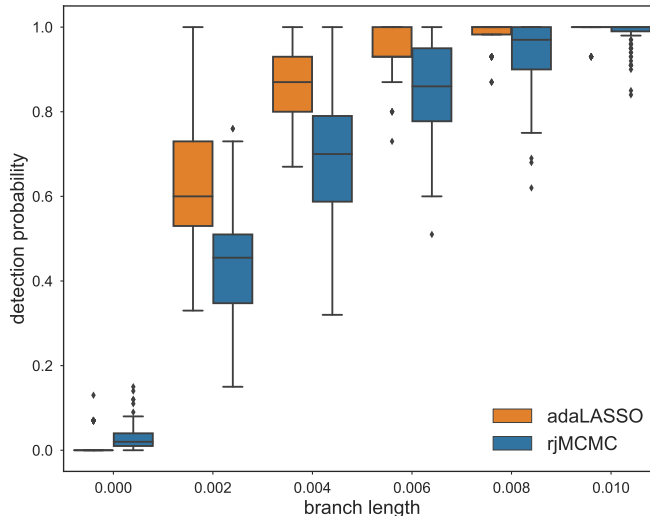


FIGURE 4. Performance of multistep (4 cycle) adaptive phylogenetic LASSO and rjMCMC at detecting zero versus short branches.

statements than their resolved counterparts. However, those sparsity encouraging procedures also make it much more difficult to detect relatively short edges. To investigate how short an edge can be and still be detected by both methods, we follow Lewis et al. (2005) and simulate a series of data sets using the same tree as in Simulation 2. All branch lengths are the same as in that simulation except those for the 15 randomly chosen short branches, each of which we take to be 0.0, 0.002, 0.004, 0.006, 0.008, 0.010 for the various trials; the nonzero short branches are meant to be particularly challenging to distinguish from the actual zero branches. For each of these six lengths, we simulate 100 data sets of the same size (1000 sites). These values for short branches are multiples of 1/1000, which provides, on average, one mutation per data set along the branch of interest. Note that branch lengths represent the expected amount of mutation per site, so a branch length of 0.001 does not guarantee that a mutation will occur on the branch of interest in every simulated data set. We run multistep adaptive phylogenetic LASSO with $M = 4$ cycles and initial regularization coefficient $\lambda^{[0]} = 50$, and rjMCMC with the polytomy prior (with $C = 1$) for analysis. The detection probabilities of rjMCMC are the averaged split posterior probabilities of the corresponding branches over the 100 independent data sets.

We find that multistep adaptive phylogenetic LASSO indeed strikes a better balance between identifying zero branches and detecting short branches than rjMCMC in this simulation study (Figure 4). In addition to being slightly better at identifying zero branches than rjMCMC (partly due to a weak polytomy prior $C = 1$), multistep adaptive phylogenetic LASSO has a substantially improved detection probability for short branches. Also note that sufficiently long branch lengths (about 10 expected substitution per data set) are usually needed for an edge to be reliably detected in either methods.

5.5. Dengue Virus Data. We now compare our adaptive phylogenetic LASSO methods to others on a real data set. So far, we have tested the performance of multistep adaptive phylogenetic LASSO on a fixed topology. For real data sets, the underlying phylogenies are unknown and hence have to be inferred from the data. We therefore propose to use multistep adaptive phylogenetic LASSO as a sparsity-enforcing procedure after traditional maximum likelihood based inferences. In what follows, we use this combined procedure together with bootstrapping to measure edge support on a real data set of the Dengue genome sequences. In our experiment, we consider one typical subset of the 4th Dengue serotype (“DENV4”) consisting of 22 whole-genome sequences from Brazil curated by the nextstrain project (Hadfield et al., 2017) and originally sourced from the LANL hemorrhagic fever virus database (Kuiken et al., 2012). The sequence alignment of these sequences comprises 10756 nucleotide sites.

Following Lewis et al. (2005), we conduct our analysis using the following methods: (1) maximum likelihood bootstrapping columns of a sequence alignment; (2) a conventional MCMC Bayesian inference restricted to fully resolved tree topologies; (3) a reversible-jump MCMC method moving among fully resolved as well as polytomous tree topologies; (4) two combined procedures, maximum likelihood bootstrapping plus multistep adaptive phylogenetic LASSO and maximum likelihood bootstrapping plus thresholding, both allow fully bifurcating and non-bifurcating tree topologies. Maximum likelihood bootstrap analysis is performed using RAxML (Stamatakis, 2014) with 1000 replicates. The conventional MCMC Bayesian analysis is done in MrBayes (Ronquist et al., 2012) where we place a uniform prior on the fully resolved topology and Exponential ($\lambda = 10$) prior on the branch lengths. The rjMCMC analysis is run in p4 (Foster, 2004), using flat polytomy prior with $C = 1$ (C is the ratio of prior mass between trees with successive numbers of internal nodes as defined in Lewis et al. (2005)). Their code can be found at <https://github.com/Anaphory/p4-phylogeny>. For each Bayesian approach, a single Markov chain was run $8e+06$ generations after a $2e+06$ generation burn-in period. Trees and branch lengths are sampled every 1000 generations, yielding 8000 samples. Both combined procedures are implemented based on the bootstrapped ML trees obtained in (1). For multistep adaptive phylogenetic LASSO, we use $M = 4$ cycles and test different initial regularization coefficients $\lambda^{[0]} = 150, 300, 450$. We set the thresholds $\kappa = 1e-06, 5e-05, 1e-04$ for the simple thresholding method.

Figure 5 shows the consensus tree obtained from the conventional MCMC samples. Each interior edge has its index number i and its support value (expressed as percentage) s_i right above it: $\{(i) : s_i\}$. If an edge has inferred length zero then it doesn’t count in this bootstrap edge support. We see that many short edges have support below 50, which indicates the strong preference for non-bifurcating topologies. Therefore, we re-estimate the support values for all interior edges (splits) on this MCMC consensus tree using the aforementioned methods and summarize the results in Table 2. Compared to other methods, sparsity-encouraging methods rjMCMC, ML+thresholding+bootstrap and ML+adaLASSO+bootstrap tends to better identify zero edges and gives consistent detection results on edges with exactly zero support (edges 2, 10, 13 and 15). More interestingly, ML+adaLASSO+bootstrap is more conservative (in terms of zero edge identification) for less supported edges (see edges 5 and 9 for example) than ML+thresholding+bootstrap, which coincides

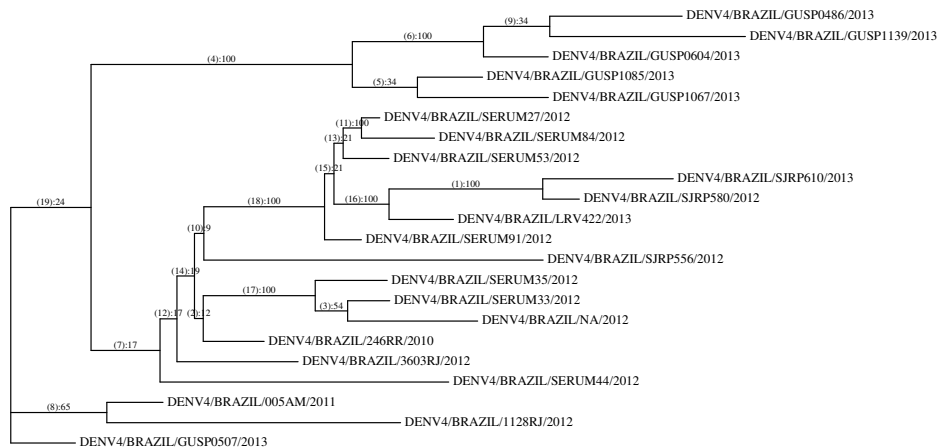


FIGURE 5. Consensus tree resulting from the conventional MCMC Bayesian inference on the Brazil clade from DENV4.

Edge	ML	MCMC	rjMCMC	ML+thresholding+bootstrap			ML+adaLASSO+bootstrap		
	bootstrap		$C = 1$	$\kappa = 1e-06$	$\kappa = 5e-05$	$\kappa = 1e-04$	$\lambda = 150$	$\lambda = 300$	$\lambda = 450$
1	100	100	100	100	100	100	100	100	100
2	7	12	0	0	0	0	0	0	0
3	93	54	1	82	65	58	66	66	66
4	95	100	100	95	95	95	95	95	95
5	38	34	1	0	0	0	4	4	4
6	63	100	100	61	61	61	63	63	63
7	10	17	20	8	8	7	6	6	6
8	52	65	31	45	44	44	44	44	44
9	11	34	1	0	0	0	2	2	2
10	10	9	0	0	0	0	0	0	0
11	61	100	66	57	56	22	61	61	61
12	13	17	3	8	2	0	3	3	3
13	9	21	0	0	0	0	0	0	0
14	23	19	3	9	2	0	4	3	4
15	13	21	0	0	0	0	0	0	0
16	99	100	100	99	99	96	99	99	99
17	94	100	100	94	94	94	94	94	94
18	88	100	100	88	88	88	88	88	88
19	6	24	24	4	4	3	3	3	3

TABLE 2. Comparison on the support values obtained from different methods on DENV4 Brazil clade data set. All analysis used the Jukes-Cantor model.

with our observation in the simulation 2. Overall, we see that (multistep) adaptive phylogenetic LASSO is able to reveal non-bifurcating structures comparable to rjMCMC Bayesian approach when applied to maximum likelihood tree topologies, and is less likely to misidentify weakly supported edges in contrast to simple thresholding.

6. CONCLUSION

We study ℓ_1 -penalized maximum likelihood approaches for phylogenetic inference, with the goal of recovering non-bifurcating tree topologies. We prove that

these regularized maximum likelihood estimators are asymptotically consistent under mild conditions. Furthermore, we show that the (multistep) adaptive phylogenetic LASSO is topologically consistent and therefore is able to detect non-bifurcating tree topologies that may contain polytomies and sampled ancestors. We present an efficient algorithm for solving the corresponding optimization problem, which is inherently more difficult than standard ℓ_1 -penalized problems with regular cost functions. The algorithm is based on recent developments on proximal gradient descent methods and their various acceleration techniques (Beck and Teboulle, 2009; O’Donoghue and Candes, 2013). As far as we know, this procedure gives the first maximum likelihood based method for non-bifurcating phylogenetic inference.

We have done a wide range of experiments to demonstrate the efficiency and effectiveness of our method. We show in a synthetic study that although the (non-adaptive) phylogenetic LASSO has difficulty finding zero-length branches, the adaptive phylogenetic LASSO provides significant improvement on sparsity recovery which validates its theoretical properties. Although assuming a fixed tree topology for deriving the statistical consistency, our method can be used to discover non-bifurcating tree topologies in real data problems when combined with traditional maximum likelihood phylogenetic inference methods. Our experiments have shown that the adaptive phylogenetic LASSO performs comparably with other MCMC based sparsity encouraging procedures (rjMCMC) in terms of sparsity recovery while being computationally more efficient as an optimization approach. We also compare our method to a heuristic simple thresholding approach and find that regularization permits more consistent performance. Finally, we show that compared to rjMCMC, the adaptive phylogenetic LASSO is more likely to detect short branches while identifying zero branches with high accuracy. It is worth mentioning that while lots of sparsity can be detected by maximizing the likelihood with non-negative constraints, the adaptive phylogenetic LASSO can be advantageous when there exist challenging zero-branches in the tree topologies with high likelihoods. Our results offer new insights into non-bifurcating phylogenetic inference methods and support the use of ℓ_1 penalty in statistical modeling with more general settings.

We leave some questions to future work. For the theory, the rate with which we can allow the number of leaves to go to infinity in terms of the sequence length is not yet known. We have also not explored the extent to which the optimal penalized tree is a contraction of the ML unpenalized tree. Also, although we have laid the algorithmic foundation for efficient penalized inference, there is further work to be done to make a streamlined implementation that is integrated with existing phylogenetic inference packages.

7. ACKNOWLEDGEMENTS

The authors would like to thank Vladimir Minin and Noah Simon for helpful discussions, and Sidney Bell for helping with the Dengue sequence data. This work supported by National Institutes of Health grants R01-GM113246, R01-AI120961, U19-AI117891, and U54-GM111274 as well as National Science Foundation grants CISE-1561334 and CISE-1564137. The research of Frederick Matsen was supported in part by a Faculty Scholar grant from the Howard Hughes Medical Institute and the Simons Foundation.

REFERENCES

- Beck, A. and M. Teboulle (2009, January). A fast iterative Shrinkage-Thresholding algorithm for linear inverse problems. *SIAM J. Imaging Sci.* 2(1), 183–202.
- Bühlmann, P. and L. Meier (2008, August). Discussion: One-step sparse estimates in nonconcave penalized likelihood models. *Ann. Stat.* 36(4), 1534–1541.
- Chen, R. and E. C. Holmes (2008, June). The evolutionary dynamics of human influenza B virus. *J. Mol. Evol.* 66(6), 655–663.
- Combettes, P. L. and V. R. Wajs (2006). Signal recovery by proximal forward-backward splitting. *Multiscale Modeling and Simulation* 4(4), 1168–1200.
- Dinh, V., L. S. T. Ho, M. A. Suchard, and F. A. Matsen IV (2016, 9 June). Consistency and convergence rate of phylogenetic inference via regularization. *arXiv; accepted to Annals of Statistics*. <http://arxiv.org/abs/1606.03059>.
- Dinh, V. C., L. S. Ho, B. Nguyen, and D. Nguyen (2016). Fast learning rates with heavy-tailed losses. In *Advances in Neural Information Processing Systems*, pp. 505–513.
- Efron, B., T. Hastie, I. Johnstone, and R. Tibshirani (2004). Least angle regression. *Annals of Statistics* 32(2), 407–499.
- Evans, S. N. and T. P. Speed (1993, March). Invariants of some probability models used in phylogenetic inference. *Ann. Stat.* 21(1), 355–377.
- Foster, P. G. (2004). Modeling compositional heterogeneity. *Syst. Biol.* 53, 485–495.
- Gardy, J., N. J. Loman, and A. Rambaut (2015, July). Real-time digital pathogen surveillance — the time is now. *Genome Biol.* 16(1), 155.
- Gavryushkina, A., T. A. Heath, D. T. Ksepka, T. Stadler, D. Welch, and A. J. Drummond (2016, August). Bayesian Total-Evidence dating reveals the recent crown radiation of penguins. *Syst. Biol.*
- Gavryushkina, A., D. Welch, T. Stadler, and A. J. Drummond (2014, December). Bayesian inference of sampled ancestor trees for epidemiology and fossil calibration. *PLoS Comput. Biol.* 10(12), e1003919.
- Georgiou, G., G. C. Ippolito, J. Beausang, C. E. Busse, H. Wardemann, and S. R. Quake (2014, January). The promise and challenge of high-throughput sequencing of the antibody repertoire. *Nat. Biotechnol.*
- Grenfell, B. T., O. G. Pybus, J. R. Gog, J. L. N. Wood, J. M. Daly, J. A. Mumford, and E. C. Holmes (2004, January). Unifying the epidemiological and evolutionary dynamics of pathogens. *Science* 303(5656), 327–332.
- Hadfield, J., C. Megill, S. M. Bell, J. Huddleston, B. Potter, C. Callender, P. Sargulenko, T. Bedford, and R. A. Neher (2017, November). Nextstrain: real-time tracking of pathogen evolution.
- Ji, S., J. Kollár, and B. Shiffman (1992). A global Łojasiewicz inequality for algebraic varieties. *Transactions of the American Mathematical Society* 329(2), 813–818.
- Jukes, T. H. and C. R. Cantor (1969). Evolution of protein molecules. In H. N. Munro (Ed.), *Mammalian protein metabolism*, Volume 3, pp. 21–132. New York: Academic Press.
- Kleinstejn, S. H., Y. Louzoun, and M. J. Shlomchik (2003, November). Estimating hypermutation rates from clonal tree data. *J. Immunol.* 171(9), 4639–4649.
- Kuiken, C., J. Thurmond, M. Dimitrijevic, and H. Yoon (2012, January). The LANL hemorrhagic fever virus database, a new platform for analyzing biothreat viruses. *Nucleic Acids Res.* 40(Database issue), D587–92.

- Lewis, P. O., M. T. Holder, and K. E. Holsinger (2005, April). Polytomies and bayesian phylogenetic inference. *Syst. Biol.* *54*(2), 241–253.
- Lewis, P. O., M. T. Holder, and D. L. Swofford (2015, January). Phycas: Software for bayesian phylogenetic analysis. *Syst. Biol.*
- Libin, P., E. Vanden Eynden, F. Incardona, A. Nowé, A. Bezenchek, EucoHIV study group, A. Sönnnerborg, A.-M. Vandamme, K. Theys, and G. Baele (2017, August). PhyloGeoTool: interactively exploring large phylogenies in an epidemiological context. *Bioinformatics*.
- Liu, Y., Z. Zhan, J. F. Cai, D. Guo, Z. Chen, and X. Qu (2016). Projected iterative soft-thresholding algorithm for tight frames in compressed sensing magnetic resonance imaging. *IEEE Trans. Med. Imag.* *35*(9), 2130–2140.
- Loh, P.-L. (2017). Statistical consistency and asymptotic normality for high-dimensional robust m -estimators. *The Annals of Statistics* *45*(2), 866–896.
- Loh, P.-L. and M. J. Wainwright (2013). Regularized m -estimators with nonconvexity: Statistical and algorithmic theory for local optima. In *Advances in Neural Information Processing Systems*, pp. 476–484.
- Neher, R. A. and T. Bedford (2015, June). nextflu: Real-time tracking of seasonal influenza virus evolution in humans. *Bioinformatics*.
- O’Donoghue, B. and E. Candes (2013). Adaptive restart for accelerated gradient schemes. *Foundations of Computational Mathematics* *15*, 515–732.
- Ronquist, F., M. Teslenko, P. van der Mark, D. L. Ayres, A. Darling, S. Höhna, B. Larget, L. Liu, M. A. Suchard, and J. P. Huelsenbeck (2012, 22 February). MrBayes 3.2: efficient bayesian phylogenetic inference and model choice across a large model space. *Syst. Biol.* *61*(3), 539–542.
- Stamatakis, A. (2014). Raxml version 8: a tool for phylogenetic analysis and post-analysis of large phylogenies. *Bioinformatics* *30*(9), 1312–1313. doi:10.1093/bioinformatics/btu033.
- Tibshirani, R. (1996, January). Regression shrinkage and selection via the lasso. *J. R. Stat. Soc. Series B Stat. Methodol.* *58*(1), 267–288.
- Van Erven, T., P. D. Grünwald, N. A. Mehta, M. D. Reid, and R. C. Williamson (2015). Fast rates in statistical and online learning. *Journal of Machine Learning Research* *16*, 1793–1861.
- Victoria, G. D. and M. C. Nussenzweig (2012, January). Germinal centers. *Annu. Rev. Immunol.* *30*, 429–457.
- Zou, H. (2006). The adaptive lasso and its oracle properties. *Journal of the American statistical association* *101*(476), 1418–1429.

8. APPENDIX

8.1. Lemmas. Here we perform further theoretical development to establish the main theorems. We remind the reader that we will continue to assume Assumptions 2.1 and 2.2. The following lemma allows gives a lower bound on the fraction of sites with state assignments in a given set. It will prove useful to obtain an upper bound on the likelihood.

Lemma 8.1. *For any non-empty set A of single-site state assignments to the leaves, we define*

$$k_A = |\{i : \mathbf{Y}^i \in A\}|$$

There exist $c_3 > 0, c_4(\delta, n) > 0$ such that for all k , we have

$$\frac{k_A}{k} \geq c_3 - \frac{c_4}{\sqrt{k}} \quad \forall A \neq \emptyset$$

with probability at least $1 - \delta$.

Proof of Lemma 8.1. Since the tree distance between any pairs of leaves of the true tree is strictly positive, there exists $c_3 > 0$ such that $P_{q^*}(\psi) \geq c_3$ for all state assignments ψ .

Using Hoeffding's inequality, for any state assignment ψ , we have

$$\mathbb{P} \left[\left| \frac{k_{\{\psi\}}}{k} - P_{q^*}(\psi) \right| \geq t \right] \leq 2e^{-2kt^2}.$$

We deduce that

$$\mathbb{P} \left[\exists \psi \text{ such that } \left| \frac{k_{\{\psi\}}}{k} - P_{q^*}(\psi) \right| \geq t \right] \leq 2e^{-2kt^2} \cdot 4^N.$$

For any given $\delta > 0$, by choosing

$$c_4(\delta, N) = \sqrt{\frac{\log(1/\delta) + (2N + 1) \log 2}{2}}$$

and $t = c_4(\delta, N)/\sqrt{k}$ we have

$$\left| \frac{k_{\{\psi\}}}{k} - P_{q^*}(\psi) \right| \leq \frac{c_4(\delta, N)}{\sqrt{k}} \quad \forall \psi$$

with probability at least $1 - \delta$. This proves the Lemma. \square

Lemma 8.2 (Chernoff bound). *Let X be any bounded random variable with $\mu = \mathbb{E}[X]$, $\sigma^2 = \text{Var}[X]$. Let b denote an upper bound of $|X|$; there exists $C_b > 0$ such that*

$$\mathbb{P}[X - \mu \leq -t] \leq \exp\left(-\frac{t^2}{C_b \sigma^2}\right), \quad \forall t > 0.$$

and

$$\mathbb{P}[|X - \mu| \geq t] \leq 2 \exp\left(-\frac{t^2}{C_b \sigma^2}\right), \quad \forall t > 0.$$

Proof of Lemma 8.2. Define

$$\kappa(x) = \begin{cases} (e^x - 1 - x)/x^2, & \text{if } x > 0 \\ 1/2 & \text{if } x = 0. \end{cases}$$

We have $\mathbb{P}[|X - \mu| \geq t] = 0$ for $t > 2b$. Hence, we only need to consider the case when $t \leq 2b$. Applying Lemma 5.6 in Van Erven et al. (2015) for $\lambda(X - \mu)$ (which is bounded from above by $a := 2\lambda b$), we have

$$(8.1) \quad \lambda^2 \kappa(-4\lambda b) \sigma^2 \leq \log \mathbb{E}[e^{-\lambda(X-\mu)}] \leq \lambda^2 \kappa(4\lambda b) \sigma^2, \quad \forall \lambda > 0.$$

From Markov's inequality,

$$\mathbb{P}[X - \mu \leq -t] = \mathbb{P}[e^{-(X-\mu)} \geq e^t] \leq \frac{\mathbb{E}[e^{-\lambda(X-\mu)}]}{e^{\lambda t}}.$$

Using (8.1), we deduce that

$$\mathbb{P}[X - \mu \leq -t] \leq \exp(\lambda^2 \kappa(4\lambda b) \sigma^2 - \lambda t).$$

Note that $\lim_{\lambda \rightarrow 0} \lambda \kappa(4\lambda b) = 0$ and $\lim_{\lambda \rightarrow +\infty} \lambda \kappa(4\lambda b) = +\infty$. Therefore, we can choose λ_{t,σ^2} such that $\lambda_{t,\sigma^2} \kappa(4\lambda_{t,\sigma^2} b) = t/(2\sigma^2)$. Since $t \leq 2b$ and σ^2 is bounded, there exists $C_b > 0$ such that $4\kappa(4\lambda_{t,\sigma^2} b) \leq C_b$ for all $t \in [-b, b]$. Thus,

$$\mathbb{P}[X - \mu \leq -t] \leq \exp(-\lambda_{t,\sigma^2} t/2) = \exp\left(-\frac{t^2}{4\kappa(4\lambda_{t,\sigma^2} b)\sigma^2}\right) \leq \exp\left(-\frac{t^2}{C_b \sigma^2}\right).$$

The argument is similar for the upper bound on $\mathbb{P}[X - \mu \geq t]$. Combining the two estimates, we also obtain the second claim of the lemma. \square

Lemma 8.3 (Generalization bound). *There exists a constant $C(\delta, n, Q, \eta, g_0, \mu) > 0$ such that for any $k \geq 3$, $\delta > 0$, we have:*

$$\left| \frac{1}{k} \ell_k(q) - \phi(q) \right| \leq C \left(\frac{\log k}{k} \right)^{1/2} \quad \forall q \in \mathcal{T}(\mu)$$

with probability greater than $1 - \delta$.

Proof. Note that for $q \in \mathcal{T}(\mu)$, $0 \geq \ell_k(\psi) \geq -\mu$ for all state assignment ψ , we obtain

$$\text{Var} \left[\frac{1}{k} \ell_k(q) \right] \leq \frac{\mu^2}{k}.$$

Using Lemma 8.2, there exists a c_5 such that

$$\mathbb{P} \left[\left| \frac{1}{k} \ell_k(q) - \phi(q) \right| \geq y/2 \right] \leq 2 \exp\left(-\frac{y^2}{4c_5 \text{Var}[U_k(q)]}\right) \leq 2 \exp\left(-\frac{y^2 k}{4c_5 \mu^2}\right).$$

For each $q \in \mathcal{T}(\mu)$, $k > 0$, and $y > 0$, define the events

$$A(q, k, y) = \left\{ \left| \frac{1}{k} \ell_k(q) - \phi(q) \right| > y/2 \right\}$$

and

$$B(q, k, y) = \left\{ \exists q' \in \mathcal{T}(\mu) \text{ such that } \|q' - q\|_2 \leq \frac{y}{4c_2} \text{ and } \left| \frac{1}{k} \ell_k(q) - \phi(q) \right| > y \right\}$$

then $B(q, k, y) \subset A(q, k, y)$ by the triangle inequality, (3.3), and (3.4). Let

$$y = \sqrt{\frac{C \log k}{k}}$$

Since $\mathcal{T}(\mu)$ is a subset of \mathbb{R}^{2N-3} , there exist $C_{2N-3} \geq 1$ and a finite set $\mathcal{H} \subset \mathcal{T}(\mu)$ such that

$$\mathcal{T}(\mu) \subset \bigcup_{q \in \mathcal{H}} V(q, \epsilon) \quad \text{and} \quad |\mathcal{H}| \leq C_{2N-3} / \epsilon^{2N-3}$$

where $\epsilon = y/(4c_2)$, $V(q, \epsilon)$ denotes the open ball centered at q with radius ϵ , and $|\mathcal{H}|$ denotes the cardinality of \mathcal{H} . By a simple union bound, we have

$$\mathbb{P} \left[\exists q \in \mathcal{H} : \left| \frac{1}{k} \ell_k(q) - \phi(q) \right| > y/2 \right] \leq 2 \exp\left(-\frac{y^2 k}{4c_5 \mu^2}\right) C_{2N-3} / \epsilon^{2N-3}.$$

Using the fact that $B(q, k, y) \subset A(q, k, y)$ for all $q \in \mathcal{H}$, we deduce

$$\mathbb{P} \left[\exists q \in \mathcal{T}(\mu) : \left| \frac{1}{k} \ell_k(q) - \phi(q) \right| > y \right] \leq 2 \exp\left(-\frac{y^2 k}{4c_5 \mu^2}\right) C_{2N-3} / \epsilon^{2N-3}.$$

To complete the proof, we need to chose C in such a way that

$$C_{2N-3} \left(\frac{4\sqrt{k}g_0c_2}{\sqrt{C \log k}} \right)^{2N-3} \times 2 \exp \left(-\frac{C \log k}{4c_5\mu^2} \right) \leq \delta.$$

Since $k \geq 3$ and $C \geq 1$, the inequality is valid if

$$C_{2N-3} (4g_0c_2)^{2N-3} \times 2k^{\frac{2N-3}{2} - \frac{C}{4c_5\mu^2}} \leq \delta$$

and can be obtained if

$$\frac{2N-3}{2} - \frac{C}{4c_5\mu^2} < 0, \quad \text{and} \quad C_{2N-3} (4g_0c_2)^{2N-3} \times 2 \cdot 3^{\frac{2N-3}{2} - \frac{C}{4c_5\mu^2}} \leq \delta.$$

In other words, we need to choose C such that

$$C \geq 4c_5\mu^2 \left(\log(1/\delta) + \log C_{2N-3} + (2N-3) \log(4\sqrt{3}g_0c_2) \right).$$

This completes the proof. \square

8.2. Technical proofs.

Lemma 2.3. *If the penalty R_k is continuous on \mathcal{T} , then for $\lambda > 0$ and observed sequences \mathbf{Y}^k , there exists a $q \in \mathcal{T}$ minimizing*

$$Z_{\lambda, \mathbf{Y}^k}(q) = -\frac{1}{k} \ell_k(q) + \lambda R_k(q).$$

Proof of Lemma 2.3. Let $\{q^n\}$ be a sequence such that

$$Z_{\lambda, \mathbf{Y}^k}(q^n) \rightarrow \nu := \inf_q Z_{\lambda, \mathbf{Y}^k}(q).$$

We note that since $\ell_k(q^*) \neq -\infty$ and R_k is continuous on the compact set \mathcal{T} , ν is finite. Since \mathcal{T} is compact, we deduce that a subsequence $\{q^m\}$ converges to some $q^0 \in \mathcal{T}$. Since the log likelihood (defined on \mathcal{T} with values in the extended real line $[-\infty, 0]$) and the penalty R_k are continuous, we deduce that q^0 is a minimizer of $Z_{\lambda, \mathbf{Y}^k}$. \square

Lemma 3.5. *For any $\mu > 0$, there exists a constant $c_2(N, Q, \eta, g_0, \mu) > 0$ such that*

$$(3.3) \quad \left| \frac{1}{k} \ell_k(q) - \frac{1}{k} \ell_k(q') \right| \leq c_2 \|q - q'\|_2$$

and

$$(3.4) \quad |\phi(q) - \phi(q')| \leq c_2 \|q - q'\|_2$$

for all $q, q' \in \mathcal{T}(\mu)$.

Proof of Lemma 3.5. Using the same arguments as in the proof of Lemma 4.2 of Dinh et al. (2016), we have

$$\left| \frac{\partial P_q(\psi)}{\partial q_i} \right| \leq \varsigma 4^n$$

for any state assignment ψ where ς is the element of largest magnitude in the rate matrix Q . By the Mean Value Theorem, we have

$$|\log P_q(\psi) - \log P_{q'}(\psi)| \leq c_2 \sqrt{2N-3} \|q - q'\|_2 \quad \forall q, q', \psi$$

where $c_2 := \varsigma 4^n / e^{-\mu}$, and $\|\cdot\|_2$ is the ℓ_2 -distance in \mathbb{R}^{2N-3} . This implies both (3.3) and (3.4). \square

Lemma 3.6. *Let G_k be the set of all branch length vectors $q \in \mathcal{T}(\mu)$ such that $\mathbb{E}[U_k(q)] \geq 1/k$. Let $\beta \geq 2$ be the constant in Lemma 3.3. For any $\delta > 0$ and previously specified variables there exists $C(\delta, N, Q, \eta, g_0, \mu, \beta) \geq 1$ (independent of k) such that for any $k \geq 3$, we have:*

$$U_k(q) \geq \frac{1}{2}\mathbb{E}[U_k(q)] - \frac{C \log k}{k^{2/\beta}} \quad \forall q \in G_k$$

with probability greater than $1 - \delta$.

Proof of Lemma 3.6. The difference of average likelihoods $U_k(q)$ is bounded by Lemma 3.5 and the boundedness assumption on \mathcal{T} , thus by Lemma 8.2 there exists $c_6 > 0$ such that

$$\mathbb{P}[U_k(q) - \mathbb{E}[U_k(q)] \leq -y] \leq \exp\left(-\frac{y^2}{c_6 \text{Var}[U_k(q)]}\right).$$

By choosing $y = \frac{1}{2}\mathbb{E}[U_k(q)] + t/2$, we have $y^2 \geq t\mathbb{E}[U_k(q)]$. For any $q \in G_k$, we deduce using (3.5) (and the fact that $\beta \geq 2$) that

$$\mathbb{P}\left[U_k(q) \leq \frac{1}{2}\mathbb{E}[U_k(q)] - t/2\right] \leq \exp\left(-\frac{c_1^2 t k \mathbb{E}[U_k(q)]}{c_2^2 c_6 \mathbb{E}[U_k(q)]^{2/\beta}}\right) \leq \exp\left(-\frac{c_1^2 t k^{2/\beta}}{c_2^2 c_6}\right).$$

For each $q \in G_k$, define the events

$$A(q, k, t) = \left\{U_k(q) - \frac{1}{2}\mathbb{E}[U_k(q)] \leq -t/2\right\}$$

and

$$B(q, k, t) = \left\{\exists q' \in G_k \text{ such that } \|q' - q\|_2 \leq \frac{t}{4c_2} \text{ and } U_k(q') - \frac{1}{2}\mathbb{E}[U_k(q')] \leq -t\right\}$$

then $B(q, k, t) \subset A(q, k, t)$ by the triangle inequality, (3.3), and (3.4). Let

$$t = \frac{C \log k}{k^{2/\beta}}.$$

To obtain a union bound and complete the proof, we need to chose C in such a way that

$$C_{2N-3} \left(\frac{4k^{2/\beta} g_0 c_2}{C \log k}\right)^{2N-3} \times 2 \exp\left(-\frac{c_1^2 C \log k}{c_2^2 c_6}\right) \leq \delta$$

where C_{2N-3} is defined as in the proof of Lemma 8.3. This can be done by choosing

$$C \geq \frac{8\beta c_2^2 c_6}{9c_1^2} \left(\log(1/\delta) + \log C_{2N-3} + (2N-3) \log(4 \cdot 3^{2/\beta} g_0 c_2)\right).$$

□

Lemma 3.8. *There exist $\mu^* > 0$ and an open neighborhood V of q^* in \mathcal{T} such that $V \subset \mathcal{T}(\mu^*)$.*

Proof of Lemma 3.8. Let

$$\mu^* = -2 \min_{\psi} \log P_{q^*}(\psi)$$

then we have $\log P_{q^*}(\psi) > -\mu^*$ for all state assignments ψ .

For a fixed value of ψ , $\log P_q(\psi)$ is a continuous function of q around q^* . Hence, there exists an neighborhood V_ψ of q^* such that V_ψ is open in \mathcal{T} and $\log P_q(\psi) >$

$-\mu^*$. Let $V = \cap_{\psi} V_{\psi}$. Because the set of all possible labels ψ of the leaves is finite, V is open in \mathcal{T} and

$$\log P_q(\psi) > -\mu^* \quad \forall \psi, \forall q \in V.$$

In other words, we have $V \subset \mathcal{T}(\mu^*)$. \square

Lemma 3.9. *If the sequence $\{\lambda_k R_k(q^*)\}$ is bounded, then for any $\delta > 0$, there exist $\mu(\delta) > 0$ and $K(\delta) > 0$ such that for all $k \geq K$, $q^{k, R_k} \in \mathcal{T}(\mu)$ with probability at least $1 - 2\delta$.*

Proof of Lemma 3.9. We first assume that $\mu > \mu^*$, where μ^* is defined in Lemma 3.8. Thus, we have $q^* \in \mathcal{T}(\mu^*) \subset \mathcal{T}(\mu)$. By definition, we have

$$-\frac{1}{k} \ell_k(q^{k, R_k}) + \lambda_k R_k(q^{k, R_k}) \leq -\frac{1}{k} \ell_k(q^*) + \lambda_k R_k(q^*)$$

which implies via Lemma 8.3 that

$$(8.2) \quad \phi(q^*) - C(\delta) \frac{\log k}{\sqrt{k}} + \lambda_k R_k(q^{k, R_k}) - \lambda_k R_k(q^*) \leq \frac{1}{k} \ell_k(q^{k, R_k})$$

with probability at least $1 - \delta$.

Let c_3 and $c_4(\delta, N)$ be as in Lemma 8.1, and assume that k is large enough such that

$$(8.3) \quad c_3 - c_4(\delta, N) \frac{\log k}{\sqrt{k}} > 0.$$

Denoting the upper bound of $\{\lambda_k R_k(q^*)\}$ by U , we define

$$\mu = \max \left\{ -2 \left(c_3 - c_4(\delta, N) \frac{\log k}{\sqrt{k}} \right)^{-1} \left(\phi(q^*) - C(\delta) \frac{\log k}{\sqrt{k}} - U \right), \mu^* \right\}.$$

If we assume that $q^{k, R_k} \notin \mathcal{T}(\mu)$, then the set $I = \{\psi : \log P_{q^{k, R_k}}(\psi) \leq -\mu\}$ is non-empty. Using Lemma 8.1, we have

$$(8.4) \quad \frac{1}{k} \ell_k(q^{k, R_k}) \leq \frac{1}{k} \sum_{Y_i \in I} \log P_{q^{k, R_k}}(Y_i) \leq -\mu \cdot \frac{k_I}{k} \leq -\mu \cdot \left(c_3 - c_4(\delta) \frac{\log k}{\sqrt{k}} \right)$$

with probability at least $1 - \delta$.

Combining equations (8.2) and (8.4), and using the fact that $\{\lambda_k R_k(q^*)\}$ is bounded by U , we obtain

$$\phi(q^*) - C(\delta) \frac{\log k}{\sqrt{k}} - U \leq -\mu \cdot \left(c_3 - c_4(\delta, N) \frac{\log k}{\sqrt{k}} \right).$$

This contradicts the choice of μ for k large enough such that (8.3) holds.

We deduce that $q^{k, R_k} \in \mathcal{T}(\mu)$ with probability at least $1 - 2\delta$. \square

8.3. More experimental results. Here we present additional experimental results for the case of $\gamma > 1$.

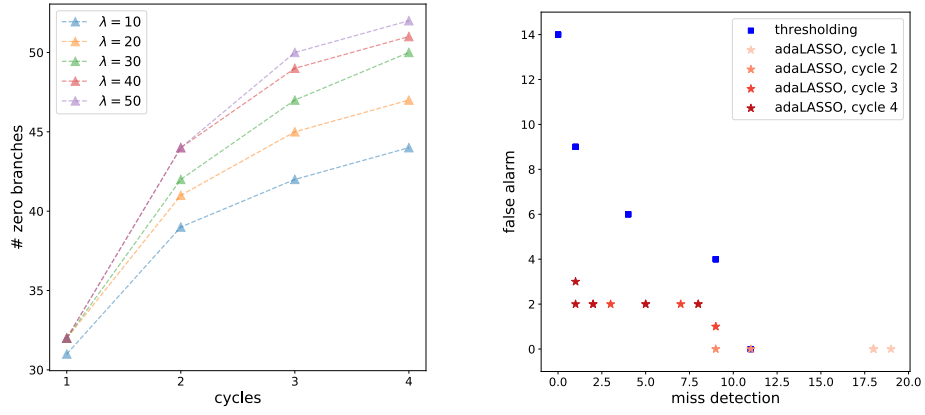


FIGURE S1. Topological consistency comparison of different phylogenetic LASSO procedures on simulation 2. $\gamma = 1.01$.

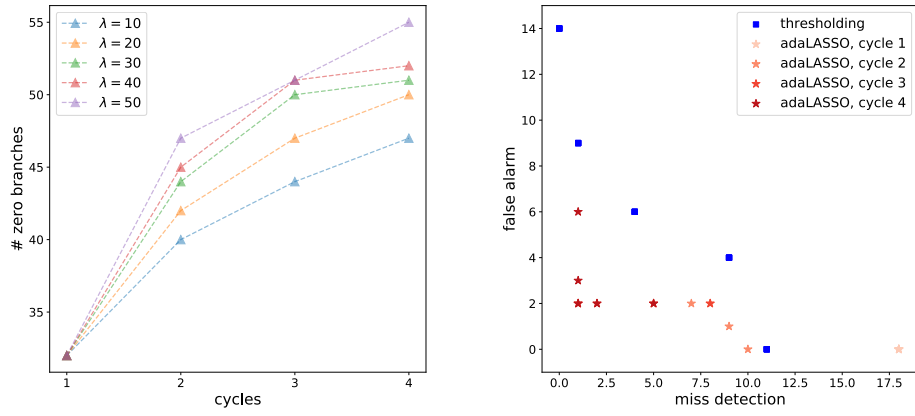


FIGURE S2. Topological consistency comparison of different phylogenetic LASSO procedures on simulation 2. $\gamma = 1.1$.

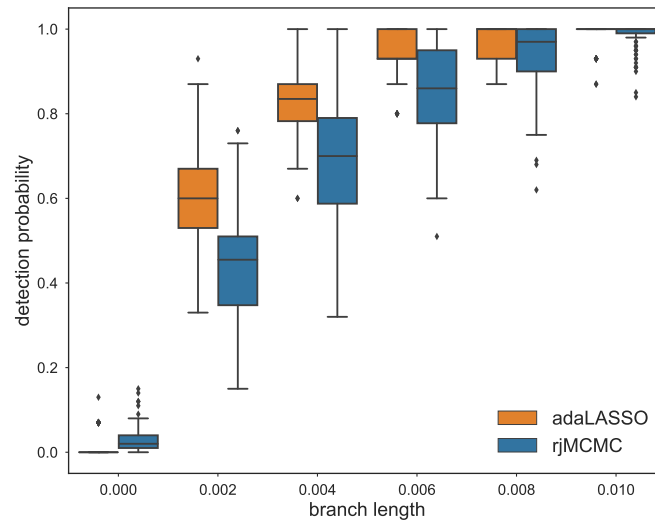


FIGURE S3. Box plot showing performance of multistep adaptive phylogenetic LASSO and rjMCMC at detecting short branches. $\gamma = 1.1$